Powder Technology 207 (2011) 26–34

Contents lists available at ScienceDirect

Powder Technology

journal homepage: www.elsevier.com/locate/powtec

Rate-dependent mechanical properties of dry blended pharmaceutical powder formulations for tabletting applications

Anuranjan Pandeya [a,*], Virendra M. Puri [b]

[a] Food Science, The Pennsylvania State University, United States
[b] Agricultural and Biological Engineering, The Pennsylvania State University, United States

ARTICLE INFO

Article history:
Received 6 July 2010
Received in revised form 29 September 2010
Accepted 1 October 2010
Available online 15 October 2010

Keywords:
Mechanical properties
Cubical triaxial tester
Pharmaceutical powder

ABSTRACT

Pharmaceutical tablets are formed using formulations consisting of ingredients such as filler, binder, disintegrant, and active pharmaceutical ingredients. In the present study, these formulations were tested to determine mechanical properties at low to medium pressure regime using a medium pressure (<10 MPa) flexible boundary cubical triaxial tester. Hydrostatic and conventional triaxial compression tests were conducted at 10 and 20 MPa/min loading rates. Fundamental elastic, elastoplastic, and rate-dependent properties such as bulk modulus, compression index, spring-back index, shear modulus, and failure stress were determined from these tests. The bulk modulus increased linearly in all cases with pressure. At 10 MPa/min loading rate, the bulk modulus value increased with the binder content. The compression index values increased with pressure in all cases of 10 and 20 MPa/min loading rates. At 10 MPa/min, the compression index generally decreased with the binder content. The spring-back index increased with the increase in pressure at both 10 and 20 MPa/min loading rates. At 10 MPa/min, the spring-back value decreased with the binder content. Shear modulus and failure stress values increased with the increase in the confining pressure. The effect of binder on failure stress values was not very prominent. These results were further used to predict the tablet quality parameters.

1. Introduction

Powder compaction is a very important unit operation for making various industrial products. Products manufactured using powder compaction include pharmaceutical tablets, cosmetic tablets, graphite electrodes, ceramic components, metal parts, coal briquettes, and sugar cubes. These products are manufactured by applying external pressure onto the powder contained in a die; which is a very rapid process. Tablet formation by applying compressive forces involves complex mechanisms during densification, i.e., compaction [7,8,20].

Pharmaceutical tablets are formed using powder formulations consisting of ingredients such as filler, binder, lubricant, disintegrant, and active pharmaceutical ingredient (API). Tablets are typically formed by blending and/or granulating these ingredients followed by lubrication and compaction. Each ingredient contributes towards tablet formation. Binder helps in granule formation as well as strengthening the tablet. Lubricant helps in reducing both die wall–particle and inter-particle friction. The function of disintegrant is to promote the disintegration of a tablet, which may influence the dissolution rate of the API and its absorption by the body.

The present 'Quality by Design' (QbD) study was initiated with a goal to study the mechanical properties of pharmaceutical powder formulations and relate these properties with tablets' quality parameters using statistical modeling. In the present paper, the mechanical properties of dry blended powder formulations determined using a flexible membrane cubical triaxial tester (CTT) is discussed. Tablet quality parameters and their relation with powders' mechanical properties will be discussed in forthcoming papers. Constitutive model parameters of modified Cam-clay model [6] were determined for mechanical characterization of powder formulations. Constitutive models have been used by various researchers to study the compaction behavior of powders. Chtourou et al. [5] developed standard calibration procedure for the cap material model for 316L stainless steel powders. The developed calibration procedure was based on a series of isostatic, triaxial and uniaxial compaction tests as well as resonant frequency tests. Lee and Kim [11] studied the densification behavior of aluminum alloy. They proposed a special form of Cap model (hyperbolic) from experimental data of Al6061 powder under triaxial compression at various loading conditions. The proposed model was implemented into a finite element program to compare with experimental data of Al alloy powder under cold compaction. Experimental data were also compared with finite element results from several other models such as Shima–Oyane; Fleck–Gurson; Cam-clay; and Drucker–Prager. Ransing et al. [22] used discrete and continuum approach to model the powder compaction

* Corresponding author.
E-mail address: azp128@psu.edu (A. Pandeya).

0032-5910/$ – see front matter © 2010 Elsevier B.V. All rights reserved.
doi:10.1016/j.powtec.2010.10.006

process. Wu et al. [25] studied the mechanical behavior of powder during compaction using the finite element method. They performed uniaxial compression experiments using a compaction simulator for their study and calibrate the Drucker–Prager Cap model. Leuenberger [12] studied the compressibility and compactibility of the powder system. He related the deformation hardness of the compact as a function of the applied pressure and the relative density. Batcher et al. [2] studied the bulk properties, compactibility and compressibility of granules produced by wet and dry granulation methods. The flow and compressibility were determined by measuring the bulk and tap density of the granules. The compactibility was estimated using the specific crushing strength. Vromans and Lerk [24] studied the effect of lubricant (magnesium stearate) on the compactibility and densification behavior of the brittle and directly compressible material. They reported that the negative effect of lubricant on the binding properties is counteracted by the facilitated densification.

Many researchers have used flexible membrane CTT for studying the mechanical behavior of powder. Li and Puri [14] used a flexible membrane CTT to measure the true three-dimensional response of powders. In their study, the compression behavior and strength of three powders: Avicel (PH 102), a spray-dried alumina powder, and a fluid-bed-granulated silicon nitride based powder were measured. Mittal and Puri [17] studied the rate-dependent mechanical properties of a dry industrial powder using CTT within the context of a new elasto-viscoplastic model (PSU-EVP model). The compression and shear properties of the powder were quantified at different compression levels. All of these research studies focused mainly on determining the mechanical properties and compaction behavior of single powder however the effect of mixing other ingredients on the properties was not studied. Hence, the present research was initiated to: (1) develop a full set of elastic, plastic, and failure properties in the low to medium pressure regime (<10 MPa) for a real pharmaceutical formulation, i.e., elastoplastic properties were measured and results reported, (2) evaluate the loading rate effect on a full set of elastoplastic properties, and (3) to determine the effect of the binder content, a critical ingredient for tablet's mechanical integrity, on the mechanical behavior of a powder mixture. The significance of measuring accurately properties in low to medium pressure range is that when tablets are formed, substantial amount of densification (i.e., void disappearance) occurs in this regime. Some estimates place it at or about 65–75% of the overall densification. Therefore, understanding of this crucial stage of densification and its impact on the final tablet quality is of considerable technical and economic importance. This paper reports the property values while the forthcoming articles will demonstrate the relationship (including a hypothesis) between select powder properties to tablet quality metrics (such as axial strength, diametral strength, hardness, and attrition).

2. Material

The formulation used for the research was composed of Avicel PH 102 (filler), Methocel (E15 Premium LV from Dow Chemicals), magnesium stearate (lubricant), Ac-Di-Sol (disintegrant), and acetaminophen (active pharmaceutical ingredient) as given in Table 1. Three different levels of methocel (binder): 0 (none), 5, and 10%, were used in powder formulation. The proportions of other four ingredients were maintained at the same level, i.e., Avicel:Acetaminophen:Ac-Di-Sol:Magnesium stearate: 0.90:0.05:0.03:0.02. The amount of binder and other ingredients was based upon the actual tablet formulation being used by the industry [23, 9]. Micrographs of formulation ingredients are shown in Fig. 1a–e. Select physical properties of ingredients are given in Table 2.

Table 1
Ingredients and their proportions used in formulation of pharmaceutical powder for dry blend and granulation.

A. Methocel (Binder)	0%	5%	10%
B. Other ingredients	100%	95%	90%
B1. Avicel PH 102	90%	85.5%	81%
B2. Acetaminophen	5%	4.75%	4.5%
B3. Ac-Di-Sol	3%	2.85%	2.7%
B4. Magnesium stearate	2%	1.9%	1.8%

3. Methodology

The ingredients were blended at different binder contents (Table 1). All the powder constituents were weighed using a balance (Acculab, readability ± 0.001 g) as per the proportion mentioned in Table 1. The powders were blended using manual Mini-Inversina (Bioengineering AG, Switzerland) capable of giving 360° motion to powder. For determining the mixing time, colored cosmetic powder was used. The size and shape of the particle size were comparable to the ingredients used in formulations. Following various trials it was visually observed that after 5 min the colored particles were uniformly distributed. Based on these trials, the mixing was performed at 80 rpm for 5 min. Hydrostatic triaxial compression (HTC) and conventional triaxial compression (CTC) tests were conducted using a flexible boundary medium pressure cubical triaxial tester (CTT). HTC tests were conducted at pressures up to 10 MPa and CTC tests were conducted at pressures up to 3 MPa. These pressures were selected to study the compression property at the low to medium pressure regime as explained earlier. Hence these pressures are much less than the pressure used by the industries for tablet formation. These tests were conducted at loading rates of 10 and 20 MPa/min to evaluate if powder has rate dependency. Initial dimension of the powder sample was 50 mm × 50 mm × 50 mm. Due to the size of the sample, at loading rates higher than 20 MPa/min, the applied pressure could not reach the center of the cubical sample. Hence, loading rates higher than 20 MPa/min was not used. Detailed description about the HTC and CTC tests are given in Pandeya [21]. The experimental design for the HTC and CTC tests is given in Tables 3 and 4, respectively. The statistical power to evaluate the individual and combined effect of variables for the HTC test was determined to be 0.8 for bulk modulus assuming a minimum effect of 10 MPa, a standard deviation of 7 and an alpha value of 0.05. The statistical power for the CTC test was determined to be 0.8 for the shear modulus assuming a minimum effect of 5 MPa, a standard deviation of 4 and an alpha value of 0.05. Details on CTT and triaxial tests can be found in Li and Puri [14,15], Mittal [16], and Pandeya [21].

4. Results and discussion

4.1. HTC test results

Bulk modulus, compression index, and spring-back index were determined from HTC tests. These parameters determined at different binder contents, pressures and loading rates are presented and discussed in the following sections.

4.2. HTC test profile

In HTC tests, the samples at binder contents of 0, 5, and 10% were unloaded and reloaded, at three different hydrostatic pressures of 2.5, 5.0 and 10.0 MPa. A typical HTC test profile for dry blended powder is shown in Fig. 2. From the figure it can be observed that the powder have limited recovery during unloading, i.e., responses were predominantly plastic. The HTC test results were evaluated for the effect of the binder and loading rate.

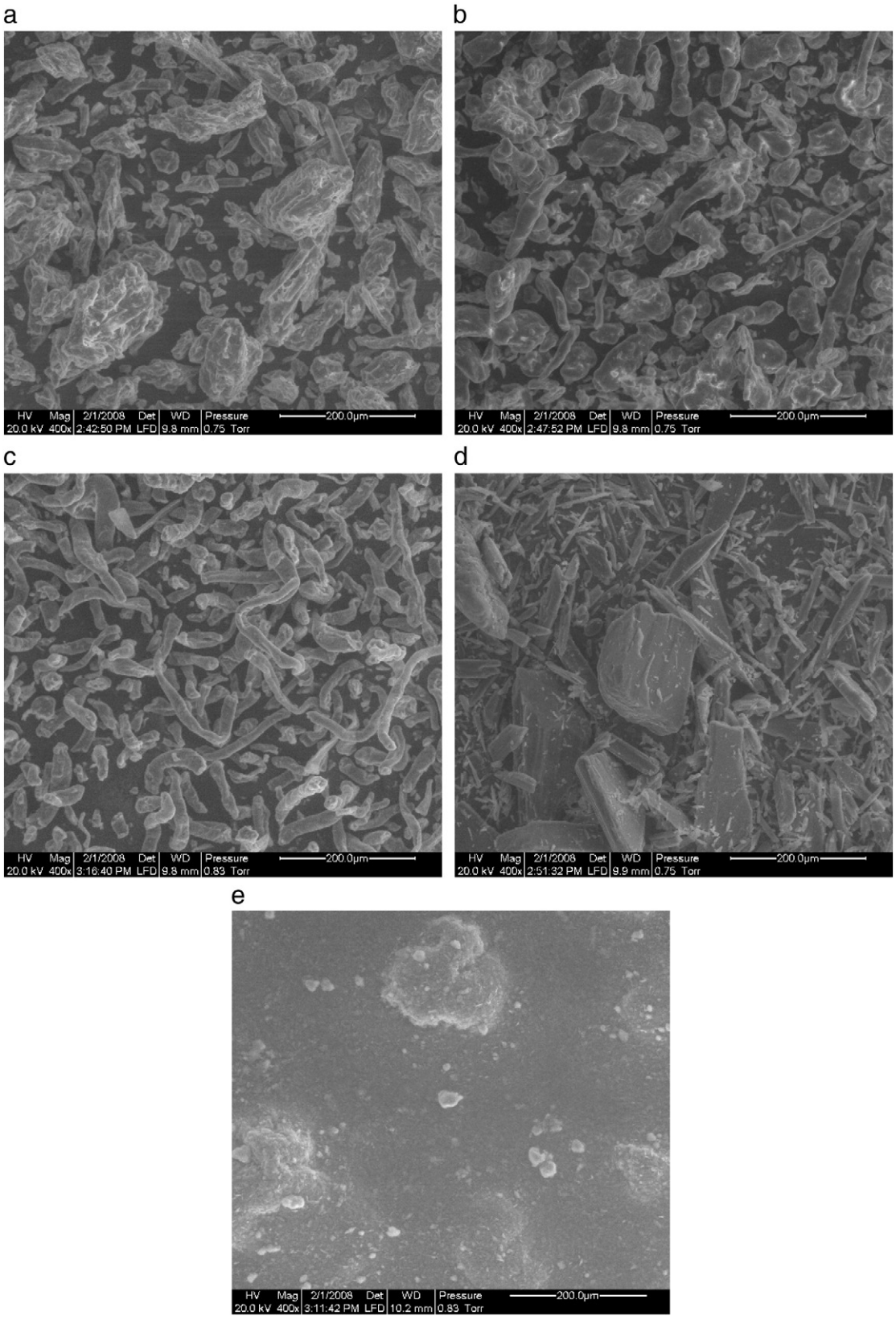

Fig. 1. Micrographs of pharmaceutical ingredients (a) Avicel, (b) Methocel, (c) Acetaminophen, (d) Ac-di-sol, and (e) Magnesium stearate.

4.3. Determination of bulk modulus, compression index, and spring-back index

Bulk modulus (K) was determined by using the HTC test results. To determine the bulk modulus at a given mean pressure, a linear regression was performed on the entire unloading and reloading curve (Fig. 2) with stress as an independent variable and strain as a dependent variable. The slope of the linear regression line gave the inverse of the bulk modulus (K) at the pressure at which the sample was unloaded.

Table 2
Select mechanical properties of formulation ingredients.

Ingredients	Parameters	
	Bulk density (g/cc)	Particle density[a] (g/cc)
Avicel PH 102	0.41	1.61
Methocel	0.42	1.33
Acetaminophen	0.25	1.36
Ac-Di-Sol	0.46	1.66
Magnesium stearate	0.26	1.13

[a] Measured using Micromeretics Multivolume Helium Pycnometer 1305 (Boynton Beach, FL).

To determine the compression index and spring-back index graph of ln (pressure) vs. void ratio was plotted. The void ratio was determined by using the change in the volume assuming that the volume change was due to change in pore space volume only. The solid volume was determined using the particle density determined using pycnometer (Table 4). The volume was estimated by measuring the change in dimension in three directions using a Linear Motion Potentiometer (LMP).

The slope of the consolidation line was used to estimate the compression index. The slope of the unloading–reloading line was used to estimate the spring-back index (Fig. 3).

4.4. Bulk modulus

At 10 MPa/min loading rate, (1) the bulk modulus increased with increase in the binder content (Fig. 4a), and (2) the average bulk modulus values at 2.5 MPa unloading pressure were 102, 116, and 136 MPa at 0, 5 and 10% binder content, respectively. These values increased to 139 (36%, percent change with respect to 2.5 MPa), 143 (23%), 170 (25%) MPa at 5.0 MPa and 215 (111%), 216 (86%) and 251 (85%) at 10.0 MPa unloading pressure. At a low loading rate (10 MPa/min), the binder had sufficient time to spread and make contact with other ingredients. Hence, with the increase in the binder content, the material had less recovery; as a result, the bulk modulus increased. The regression equations for bulk modulus vs. pressure at 10 MPa/min for various binder contents are given in Table 5. The slope of the regression line at three binder contents were nearly the same i.e. the increase in the modulus values with pressure had a similar trend.

At 20 MPa/min, (1) the bulk modulus was maximum at 0% binder followed by those at 10 and 5% binder contents (Fig. 4b) and (2) the average bulk modulus at 2.5 MPa unloading pressure were 163, 127, 145 MPa at 0, 5 and 10% binder content, respectively. These values increased to 207 (27%), 172 (35%), and 196 (35%) MPa at 5 MPa and 314 (92%), 256 (101%) and 280 (93%) at 10.0 MPa unloading pressure. To explain the behavior a hypothesis was proposed that at a high loading rate the binder particles get deformed much more compared to 10 MPa/min loading rate to create sufficient void space to be filled by the ingredients which resulted in more recovery and, hence, bulk modulus was less in the presence of binder at a higher loading rate. The regression equations for bulk modulus values vs. pressure at 20 MPa/min for various binder contents are given in Table 5. The slope of the regression line at three binder contents, as in the case of 10 Pa/min loading rate, was nearly same.

Analysis of Covariance (ANCOVA) was done to evaluate the relationship of bulk modulus with pressure at different levels of binder content and loading rate. Based on the ANCOVA neither binder content nor loading rate had a significant effect ($p>0.05$) on the bulk modulus value. In addition, slopes of the regression lines did not differ significantly ($p>0.05$). Bulk modulus did increase as a linear function of pressure.

The bulk modulus at 20 MPa/min loading rate was higher than at 10 MPa/min loading rate in all cases, which indicated that the mechanical behavior of powder formulations is rate-dependent. At a higher loading rate, the powder did not have sufficient time to respond to applied stress, i.e., the residual stress during loading continued the process of compression during unloading leading to less recovery and higher bulk modulus values. This is consistent with the time-dependent response such as creep and stress relaxation reported in the literature for particulate systems [3,4].

Table 3
Experimental design for HTC tests of powder formulations.

Stress path (MPa)	Loading rate	Binder content (%)		
		0	5	10
0.0 – 2.5 – 0.1 – 5.0 – 0.1 – 10.0 – 0.1 – 10.0 – 0	10 MPa/min	3	3	3
	20 MPa/min	3	3	3

Table 4
Experimental design for CTC tests.

Loading rate (MPa/min)	CP (MPa)	Stress path (MPa)	Binder content (%)		
			0	5	10
10	1	0.0 – 1.0 – 0.0 – 1.0 – 0.0	3[a]	3	3
	2	0.0 – 1.0 – 0.0 – 2.0 – 0.0 – 2.0 – 0.0	3	3	3
	3	0.0 – 1.0 – 0.0 – 2.0 – 0.0 – 2.0 – 0.0	3	3	3
20	1	0.0 – 1.0 – 0.0 – 1.0 – 0.0	3	3	3
	2	0.0 – 1.0 – 0.0 – 2.0 – 0.0 – 2.0 – 0.0	3	3	3
	3	0.0 – 1.0 – 0.0 – 2.0 – 0.0 – 2.0 – 0.0	3	3	3

CP — confining pressure.
[a] Number of replicates.

4.5. Compression index

The compression index, an elastoplastic parameter, is the measure of compressibility of the material using void ratio as the dependent variable. Compression index incorporates both elastic and plastic deformations. For a given formulation, the magnitudes of these elastic vs. plastic contributions change with regime and rate of loading. In all cases, the compression index value increased with pressure (Fig. 5a and b). Similar trend was observed by Li [13] for micro-crystalline cellulose (MCC). Mittal and Puri [19] also observed similar trend for MCC up to 9 MPa pressure. In the present research, the formulation contained 80 to 90% MCC, which appears to dominate the results.

At 10 MPa/min loading rate, the average compression index values for 0% binder were 0.460, 0.577 (25.4%, percent change with respect to 2.5 MPa) and 0.787 (71.0%) at 2.5, 5.0 and 10 MPa unloading pressures, respectively (Fig. 5a). These values were 0.283, 0.579 (104.5%), and 0.699 (146.9%) for 5% binder content and 0.250, 0.537 (114.8%) and 0.726 (190.4%) for 10% binder content. Based on the values, the material became more compressible with an increase in pressure. The powder formulations contained irregular shaped

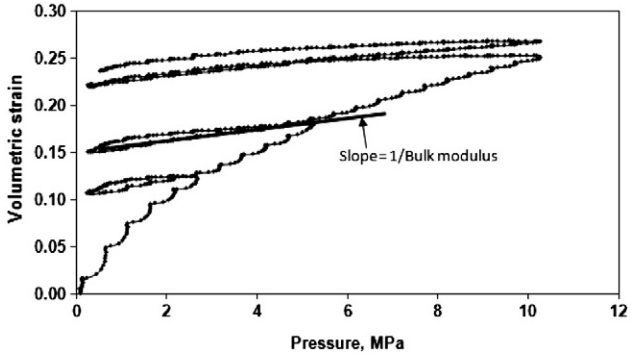

Fig. 2. Typical HTC response at a loading rate of 10 MPa/min and a binder content of 5%.

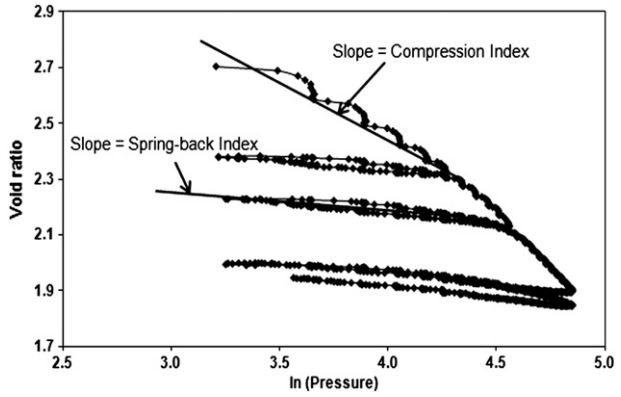

Fig. 3. ln(pressure) vs. void ratio plot for determination of compression and spring-back index.

ingredients such as MCC (81–90%), methocel, and acetaminophen which have needle-like shape (Fig. 1). Due to irregular shapes, the particle rearrangement continued throughout the pressure loading regime of 10 MPa. The compression index was higher for powder formulation without binder compared to powder formulations having 5 and 10% binder at 2.5 MPa pressure, which means that powders with binder were more resistant to void ratio change due to the presence of binder. The compression index in the case of 5 and 10% binder were very close, which indicated that increasing the binder from 5 to 10% had a limited effect.

Table 5
Regression equation for predicting bulk modulus at 10 MPa/min and 20 MPa/min.

Binder, %	Regression equation	
	10 MPa/min	20 MP/min
0	$BM = 15*P + 64.0$ ($r^2 = 0.98$)	$BM = 20*P + 110.0$ ($r^2 = 0.93$)
5	$BM = 13*P + 79.9$ ($r^2 = 0.98$)	$BM = 17*P + 84.8$ ($r^2 = 0.87$)
10	$BM = 15*P + 95.9$ ($r^2 = 0.91$)	$BM = 17*P + 103.1$ ($r^2 = 0.72$)

BM — bulk modulus (MPa); P — pressure (MPa).

At 20 MPa/min loading rate, as in the case of 10 MPa/min, compression index increased with increase in pressure. The average compression index values for 0% binder were 0.345, 0.485 (40.5%) and 0.632 (83.1%) at 2.5, 5.0 and 10 MPa unloading pressure, respectively (Fig. 5b). These values were 0.279, 0.530 (89.9%), and 0.695 (149.1%) for 5% binder and 0.280, 0.500 (78.5%) and 0.651 (132.5%), respectively, for 10% binder.

In general, the compression index values were higher at 10 MPa/min compared to those at 20 MPa/min loading rate. This difference was more in the case of 0% binder content. At 10 MPa/min the powder had more time to respond to the applied load, and hence was more compressible, resulting in a higher compression index. Similar trend has been observed by Huang and Puri [10] for MCC at pressures up to 3 MPa.

Compression index was analyzed for interaction at different level of binder contents, pressure, and loading rates. Tukey comparison was performed between the mean values of compression index using Minitab to evaluate the effect of pressure, binder content and loading rate. Based on the ANOVA table pressure, binder content, and loading rate together did not have a significant effect ($p > 0.05$) on the compression index value. However, treatment combinations of binder content and pressure, binder content and loading rate, and pressure and loading rate were significant ($p < 0.05$).

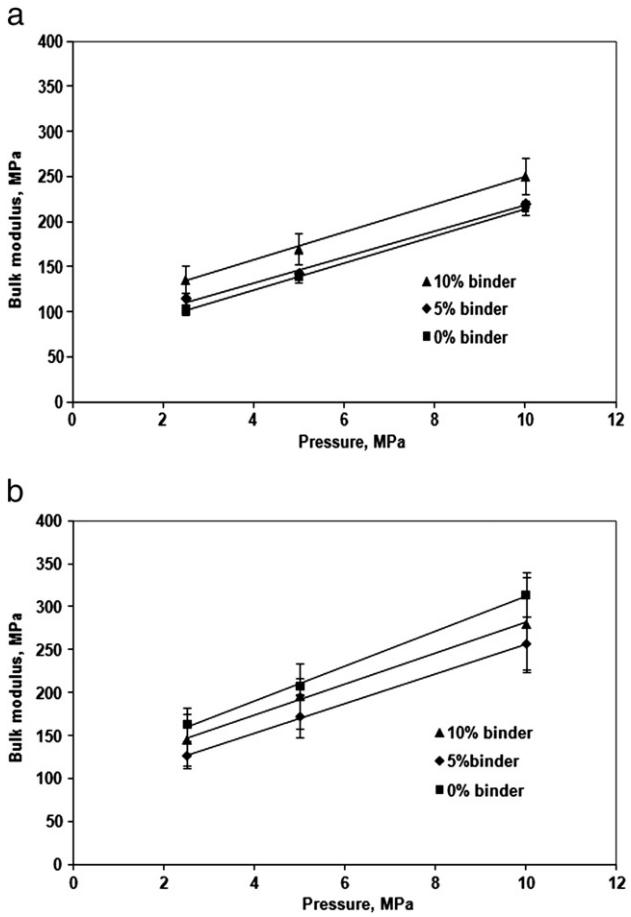

Fig. 4. Bulk modulus of powder formulations at (a) 10 MPa/min loading rate and three binder contents and (b) 20 MPa/min loading rate and three binder contents.

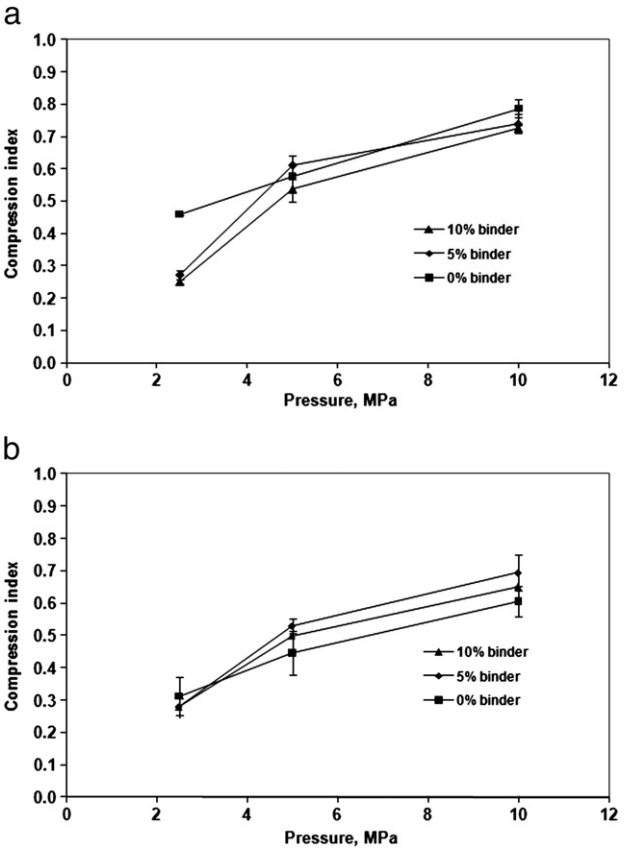

Fig. 5. Compression index of powder formulations at (a) 10 MPa/min loading rate and three binder contents and (b) at 20 MPa/min loading rate and three binder contents.

4.6. Spring-back index

Spring-back index, an elastic parameter, is the measure of elastic recovery of the material's void ratio after the applied pressure during HTC loading has been released. In all cases, the spring-back index value increased with pressure (Fig. 6a and b). With an increase in pressure, the powder formulation particles became more stable and gained strength which resulted in the solid-like behavior of powder formulation, i.e. greater elastic response as reflected in the spring-back index values. Similar trends were observed by Li [13] for MCC, alumina, and silicon nitride. Mittal and Puri [19] reported similar result for silicon nitride.

At 10 MPa/min loading rate, the spring-back index values decreased with the binder content (Fig. 6a). The binder material being soft and more plastic, reduced the elastic recovery of the powder hence the spring-back index declined with an increase in the binder content. The average spring-back index values for 0% binder were 0.090, 0.096 (6.7%) and 0.109 (21.4%) at 2.5, 5.0 and 10 MPa unloading pressure, respectively. These values were 0.064, 0.083 (29.7%), and 0.096 (50.0%) respectively for 5% binder and 0.066, 0.080 (21.7%) and 0.094 (43.5%), respectively for 10% binder. The regression equations for the spring-back index values at 10 MPa/min for various binder contents are given in Table 6.

At 20 MPa/min the spring-back index values were the lowest at 0% binder followed by 10 and 5% binder content (Fig. 6b). The average spring-back index values for 0% binder were 0.050, 0.057 (15.5%) and 0.070 (41.41%) at 2.5, 5.0 and 10 MPa unloading pressure, respectively. These values were 0.065, 0.075 (14.5%), and 0.081 (24.3%), respectively for 5% binder and 0.059, 0.068 (14.6%), and 0.079, respectively for 10% (33.0%) binder. The regression equations for spring-back index values vs. pressure at 20 MPa/min for various binder contents are given in Table 6. No clear trend for the effect of binder was observed at 20 MPa/min.

Table 6
Regression equation for predicting spring-back index at 10 and 20 MPa/min.

Binder, %	Regression equation	
	10 MPa/min	20 MPa/min
0	$SI = 0.003^*P + 0.0830$ ($r^2 = 0.85$)	$SI = 0.003^*P + 0.0431$ ($r^2 = 0.90$)
5	$SI = 0.004^*P + 0.0577$ ($r^2 = 0.89$)	$SI = 0.002^*P + 0.0622$ ($r^2 = 0.32$)
10	$SI = 0.004^*P + 0.0586$ ($r^2 = 0.81$)	$SI = 0.003^*P + 0.0538$ ($r^2 = 0.29$)

SI — spring-back index; P — pressure (MPa).

The relationship of the spring-back index with pressure was analyzed at different levels of binder content and loading rate. Based on the ANCOVA table, neither binder content nor loading rate had a significant effect ($p > 0.05$) on slopes of the regression lines, i.e., slopes did not differ significantly. Therefore, it was a case of common slope model and Tukey mean comparisons were performed. The binder*-loading rate interaction was significant ($p < 0.05$).

The spring-back index values were higher at 10 MPa/min loading rate as compared to 20 MPa/min loading rate. This difference was largest in the case of 0% binder. At 10 MPa/min loading rate, the powder particle had more time to respond to the applied force as a result the applied force reached up to the center of the sample and gained more strength compared to 20 MPa/min loading rate. This resulted in more decrease in void space at 10 MPa/min loading condition and increase in solid-like behavior and, consequently, greater elastic recovery response.

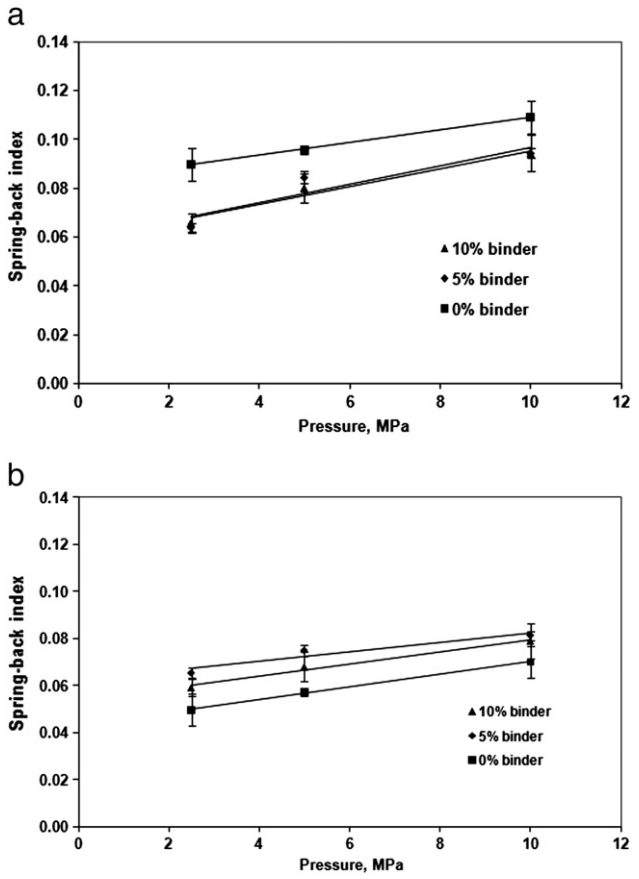

Fig. 6. Spring-back index of dry blended powder formulations (a) at 10 MPa/min loading rate and three binder contents and (b) at 20 MPa/min loading rate and three binder contents.

4.7. CTC test profile

In CTC tests, the samples at binder contents of 0, 5, and 10% were unloaded and reloaded up to a stress difference of 2 MPa, at three confining pressures of 1, 2 and 3 MPa. A typical CTC test profile for powder formulation is shown in Fig. 7. From these CTC profiles, as the confining pressure increased, the strain difference decreased. The effect of binder on the strain difference values was not very prominent. The strain difference at 20 MPa/min loading rate was more than at 10 MPa/min loading rate in the case of 1 MPa confining pressure.

4.8. Shear modulus

The shear modulus (G) is the measure of resistance of the material to deformation in shear loading. At 10 MPa/min loading rate and stress difference of 1 MPa, the average shear modulus values at

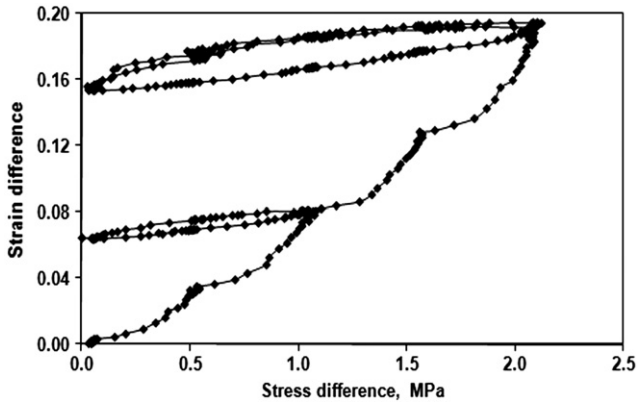

Fig. 7. Typical CTC response at 2 MPa confining pressure and 10 MPa/min loading rate for binder content 10%.

1.0 MPa confining pressure were 13, 18, and 18 MPa at 0, 5 and 10% binder content, respectively. These values increased to 31 (72%, percent change from the 1.0 MPa confining pressure value), 30 (66%), 30 (25%) MPa at 2.0 MPa and 36 (176%), 37 (105%) and 33 (83%) at 3.0 MPa confining pressures (Fig. 8a). The average shear modulus values at a stress difference of 2 MPa and 2.0 MPa confining pressure were 25, 26, and 26 MPa at 0, 5, and 10% binder content, respectively. These values at 3.0 MPa confining pressure were 37 (48%, percent change from 2 MPa confining pressure), 35 (35%), and 34 (30%) MPa, respectively (Fig. 8a). The shear modulus increased with increase in the confining pressure in all cases. With increase in confining pressure, the strength of the sample increased, and hence, the resistance to deformation increased as a result the shear modulus increased. An increase in shear modulus with pressure has also been reported by earlier researchers [10,13,18,19]. Chtourou et al. [5] also reported an increase in shear modulus with an increase in relative density.

At 20 MPa/min loading rate and stress difference of 1 MPa, the average shear modulus values at 1.0 MPa confining pressure were 26, 28, and 28 MPa at 0, 5 and 10% binder content, respectively. These values increased to 35 (35%), 32 (14%), 30 (7%) MPa at 2.0 MPa and 37 (42%), 36 (29%) and 35 (25%) at 3.0 MPa confining pressures (Fig. 8b). The average shear modulus values at a stress difference of 2 MPa and 2.0 MPa confining pressure were 28, 25, and 24 MPa at 0, 5 and 10% binder content, respectively. These values at 3.0 MPa confining pressure were 30, 32, and 34 MPa, respectively. Similar to the case of 10 MPa/min loading rate, the shear modulus increased with an increase in the confining pressure in all cases. No clear trend of the effect of binder on shear modulus values was observed unlike bulk modulus. The hypothesis proposed to explain the behavior was that binder in dry form spreads and fills the void spaces. In the case of HTC tests, the hydrostatic pressure compressed the sample from all directions and binder under pressure spread and filled the void spaces. In the case of CTC tests, the pressure is applied differently in the form of deviatoric stress; as a result binder could not spread and fill the void spaces.

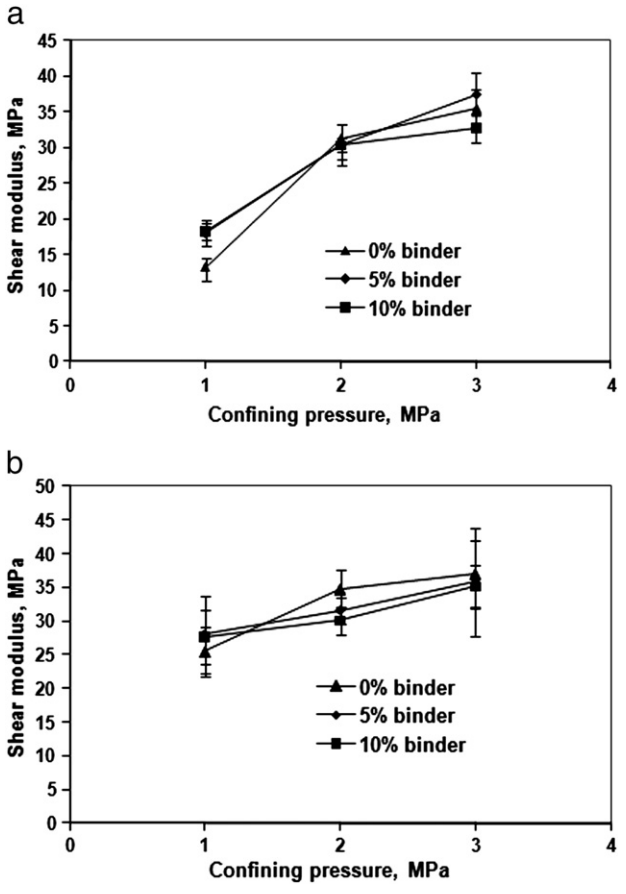

Fig. 8. Shear modulus of dry blended powder formulations at 1 MPa stress difference and three binder contents at loading rates of (a) 10 MPa/min and (b) 20 MPa/min.

Tukey comparison was performed between the mean values of shear modulus using Minitab to evaluate the effect of pressure, binder content, and loading rate. Based on the ANOVA table, pressure, binder content, and loading rate together did not have a significant effect ($p>0.05$) on shear modulus values. However, treatment combination of pressure and loading rate was significant ($p<0.05$).

The shear modulus values at 10 and 20 MPa/min loading rate were different, which indicated that the formulations were rate-dependent. However, no clear trend of the effect of loading rate was observed. Other researchers also observed variation in shear modulus values with loading rates. Huang and Puri [10] observed decrease in shear modulus value with strain rate. Mittal [16] also observed decrease in shear modulus with compression rate. In general, the shear modulus increased with loading rate at 1 MPa stress difference. The results were different from results reported by other researchers. This may be due to the use of formulation containing lubricants and binder instead of single powder. The shear modulus values at 2 MPa stress difference were only marginally different at the two loading rates.

4.9. Failure stress and critical state line

The stress difference value at failure (failure stress) was determined at a strain difference value of 14%. In some cases of 3 MPa confining pressure, the 15% strain difference value [1] was not reached hence for uniformity, the stress value at 14% strain difference value was taken as the failure point. The failure stress value increased with confining pressure in all cases. The modified Cam-clay model assumes that the critical state line (fixed yield surface), a plot between mean pressure and failure stress, is a straight line passing through the origin. However, in the present case the line was not linear. Therefore, using Mittal and Puri's [17] mathematical formulation, the critical state line equation was obtained using a power law representation passing through the origin.

At 10 MPa/min loading rate, the average stress difference values at failure point for 1.0 MPa confining pressure were 0.95, 1.01, and 1.02 MPa at 0, 5, and 10% binder content, respectively. These values increased to 1.81 (103%, percent change from 1 MPa value), 1.71 (80%), 1.69 (72%) MPa at 2.0 MPa and 1.97 (111%), 1.99 (92%) and 1.88 (76%) at 3.0 MPa confining pressures (Fig. 9a). The equations of critical state line at different binder contents are given in Table 7. Increases in failure stress value with confining pressure are also reported by other researchers [10,13,16].

At 20 MPa/min loading rate, the average failure stress values at 1.0 MPa confining pressure were 1.33, 1.42, and 1.38 MPa at 0, 5 and 10% binder content, respectively. These values increased to 1.84 (38%, percent change from 1 MPa value), 1.82 (29%), 1.83 (32%) MPa at 2.0 MPa and 1.90 (43%), 1.95 (38%) and 1.99 (44%) at 3.0 MPa confining pressures (Fig. 9b). The equation of the critical state line at different binder contents is given in Table 7.

The failure stress values at 10 and 20 MPa/min loading rate were different at a confining pressure of 1 MPa. At 2 and 3 MPa confining pressures, these values were very close. Mittal [16] also reported that failure stress values at different loading rates were very close.

Tukey comparison was performed between the mean values of failure stress to evaluate the effect of pressure, binder content and loading rate. Based on the ANOVA table, pressure, binder content, and loading rate together did not have a significant effect ($p>0.05$) on failure stress values. However, treatment combination of pressure and loading rate was significant ($p<0.05$).

The result of the research has wide application in industry involved in powder compaction especially pharmaceutical. Previous

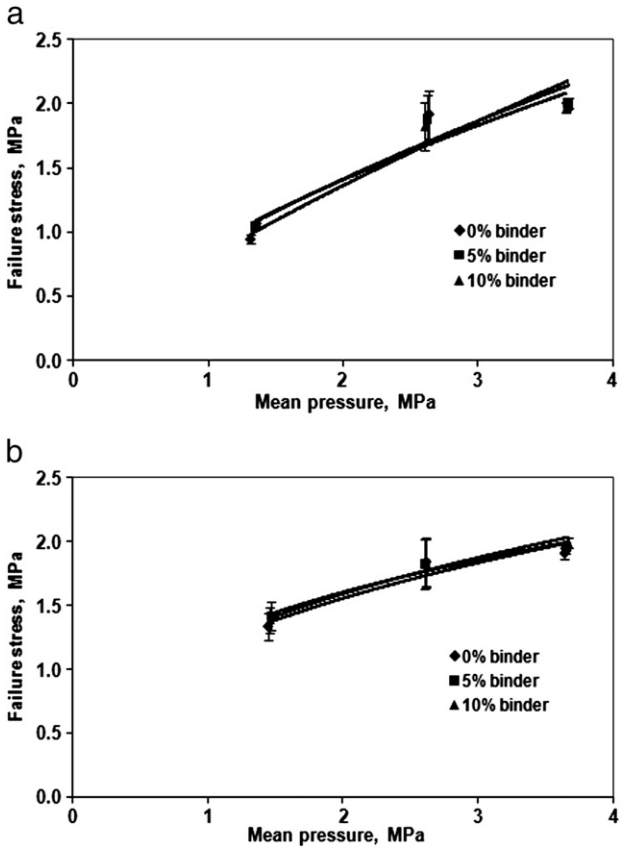

Fig. 9. Failure stress and fixed yield surface of dry blended powder formulations for different binder contents at loading rates of (a) 10 MPa/min and (b) 20 MPa/min.

works reported in this area were mostly mechanical properties of single powder however, powder compaction in industries including pharmaceutical is done in mixed form consisting of various ingredients. In this study, emphasis was on the role of the binder content on powder mixture's response and the effect on full range of elastic, plastic, and failure properties. The compression behavior of the powder can be evaluated using the CTT at a low pressure regime for different formulations and can be used for optimizing the formulation suitable for the desired quality. For e.g. in the present research the effect of binder was evaluated. In the case of the spring-back index the value does not change when the binder content changed from 5 to 10%. Subsequently, in the research the tablets were formed using same formulation and their quality parameters were determined. These tablets demonstrated a similar effect with respect to binder i.e. the quality do not change much when the binder content changed from 5 to 10%. The powders' mechanical properties related well with the tablet quality and statistical relationships were developed between the two with $r^2>0.8$. (Tablet quality and its relationship with powders' property will be discussed in detail in forth coming paper). Also, the powder formulation was found to be rate-dependent i.e. mechanical properties had different values at different loading rates which mean that the rate of application of pressure or force has its effect on the tablet quality.

Table 7
Critical state line equation at 10 and 20 MPa/min loading rates.

Binder content, %	Critical state line equation	
	10 MPa/min	20 MPa/min
0	$FS=0.870^{*}(MP)^{0.634}$ ($r^2=0.96$)	$FS=1.119^{*}(MP)^{0.416}$ ($r^2=0.93$)
5	$FS=0.846^{*}(MP)^{0.685}$ ($r^2=0.98$)	$FS=1.216^{*}(MP)^{0.359}$ ($r^2=0.96$)
10	$FS=0.796^{*}(MP)^{0.751}$ ($r^2=0.95$)	$FS=1.211^{*}(MP)^{0.370}$ ($r^2=0.98$)

5. Conclusions

Pharmaceutical powder formulations were tested to quantify fundamental mechanical properties. HTC and CTC tests were conducted using a flexible boundary medium pressure CTT. Bulk modulus, compression index, spring-back index, shear modulus and failure stress were determined at different binder contents and loading rates. The results obtained are summarized below:

Bulk modulus increased linearly in all cases with pressure from 2.5 to 10.0 MPa. Different results were obtained for different loading rates which showed that the powder formulations were a rate-dependent material. The bulk modulus value increased with the binder content at 10 MPa/min loading rate. Based on the ANCOVA neither binder content nor loading rate had a significant effect ($p>0.05$) on bulk modulus value. Bulk modulus did increase as a linear function of pressure.

Compression index values increased with pressure in all cases. At 10 MPa/min loading rate, the compression index generally decreased with the binder content. Based on the ANOVA table pressure, binder content, and loading rate together did not have a significant effect ($p>0.05$) on the compression index value. However, treatment combinations of binder content and pressure, binder content and loading rate, and pressure and loading rate were significant ($p<0.05$).

The spring-back index increased with the increase in pressure in all cases. At 10 MPa/min loading rate, the spring-back value decreased with the binder content. At 20 MPa/min the value was lowest at 0% binder followed by 10 and 5% binder content. Based on the ANCOVA table, neither binder content nor loading rate had a significant effect ($p>0.05$) on the slopes of the regression lines. Tukey mean comparisons were performed and binder–loading rate interaction was found significant ($p<0.05$).

Shear modulus increased with an increase in the confining pressure in all cases. No clear trend of the effect of binder on shear modulus values was observed. Based on the ANOVA table, pressure, binder content, and loading rate together did not have a significant effect ($p>0.05$) on shear modulus values. However, treatment combination of pressure and loading rate was significant ($p<0.05$).

Failure stress value increased with an increase in the confining pressure in all cases. The effect of binder on failure stress values was not very prominent. The failure stress was different at two loading rates; however, no clear trend was observed. Based on the ANOVA table, pressure, binder content, and loading rate together did not have a significant effect ($p>0.05$) on failure stress values. However, treatment combination of pressure and loading rate was significant ($p<0.05$).

References

[1] ASTM 1995. Annual Book of ASTM Standards (1995). Soil and rock (I): 04.08. D420–D4914.
[2] C. Bacher, P.M. Olsen, P. Bertelsen, J.M. Sonnergaard, Compressibility and compactibility of granules produced by wet and dry granulation, International Journal of Pharmaceutics 358 (1–2) (2008) 69–74.
[3] R.G. Bock, V.M. Puri, H.B. Manbeck, Triaxial test sample size effect on stress relaxation of wheat en masse, Transactions of the ASABE 34 (4) (1991) 966–971.
[4] W.F. Chen, G.Y. Baladi, Soil plasticity: Theory and Applications, Elsevier, NY, 1985.
[5] H. Chtourou, M. Guillot, A. Gakwaya, Modeling of the metal powder compaction process using the cap model. Part I. Experimental material characterization and validation, International Journal of Solids and Structures 39 (2002) 1059–1075.
[6] C.S. Desai, H.J. Siriwardane, Constitutive Laws for Engineering Materials with Emphasis on Geological Materials, Prentice Hall, Englewood Cliffs, NJ., 1984
[7] E. Doelker, Assessment of powder compaction, Powder Technology and Pharmaceutical Processes (Handbook of Powder Technology, Volume 9), Dominique Chulia, Elsevier, NY, 1993.
[8] R.M. German, Powder metallurgy science, Second EditionMetal Powder Industries Federation, Princeton, NJ, 1994.
[9] http://www.fmcbiopolymer.com/Pharmaceuticals/ToolKit/PharmaceuticalProblemSolver/tabid/836/Default.aspx. Accessed on June 19, 2008.

[10] L. Huang, V.M. Puri, Determination of time-dependent constitutive model parameter determination for microcrystalline cellulose, Particulate Science and Technology 18 (1) (2000) 9–24.
[11] S.C. Lee, K.T. Kim, Densification behavior of aluminum alloy powder under cold compaction, International Journal of Mechanical Sciences 44 (2002) 295–1308.
[12] H. Leuenberger, The compressibility and compactibility of powder systems, International Journal of Pharmaceutics 12 (1) (1982) 41–55.
[13] F., Li, 1999. Mechanical behavior of powders: tester design, load–response measurement and constitutive modeling. Ph.D. Dissertation. The Pennsylvania State University, University Park, PA.
[14] F. Li, V.M. Puri, Mechanical behavior of powders using a medium pressure flexible boundary cubical triaxial tester, Proceedings of Institution of Mechanical Engineers J. Process Mechanical Engineering 217 (E) (2003) 233–241.
[15] F. Li, and V.M. Puri. 1997. Development, testing, and verification of a medium pressure flexible boundary cubical triaxial tester. ASAE Paper No. 97-4104, American Society of Agricultural Engineers, St. Joseph, MI.
[16] B. Mittal 2003. An elasto-viscoplastic constitutive formulation for dry powder compression analysis using finite elements. PhD dissertation. Univ Park, PA: The Pennsylvania State University, Department of Agricultural and Biological Engineering.
[17] B. Mittal, V.M. Puri, Rate-dependent elasto-viscoplastic constitutive model for industrial powders. Part 1: Parameter quantification, Particulate Science and Technology 23 (2005) 249–264.
[18] B. Mittal, V.M. Puri, An elasto-viscoplastic constitutive model incorporating pore air compressibility during powder compaction process, Particulate Science and Technology 21 (2) (2003) 131–155.
[19] B. Mittal, V.M. Puri, Correlations between powder deposition methods and green compaction quality: Part I: Mechanical properties of powders, Particulate Science and Technology 17 (1999) 283–299.
[20] D.E. Niesz, A review of ceramic powder compaction, KONA (Powder and Particle) 14 (1996) 44–51.
[21] A. Pandeya, 2009. Relating mechanical properties of dry and granulated pharmaceutical powder formulations with tablet quality parameters. Ph.D. Dissertation. The Pennsylvania State University, University Park, PA.
[22] R.S. Ransing, D.T. Gethin, A.R. Khoei, P. Mosbah, R.W. Lewis, Powder compaction modelling via the discrete and finite element method, Materials and Design 21 (2000) 263–269.
[23] Q. Singh, H. Patel, M. Cassim, Comparative evaluation of tablet formulation, June 19, 2008 http://www.ru.ac.za/academic/departments/pharmacy/jrats/vol1_1/poster6/tablet8.html. Accessed on.
[24] H. Vromans, C.F. Lerk, Densification properties and compactibility of mixtures of pharmaceutical excipients with and without magnesium stearate, International Journal of Pharmaceutics 46 (3) (1988) 183–192.
[25] C.-Y. Wu, O.M. Ruddy, A.C. Bentham, B.C. Hancock, S.M. Best, J.A. Elliot, Modeling the mechanical behavior of pharmaceutical powders during compaction, Powder Technology 152 (2005) 107–117.